Aerospace Science and Technology 132 (2023) 108044

Contents lists available at ScienceDirect

Aerospace Science and Technology

journal homepage: www.elsevier.com/locate/aescte

A low-frequency micro-vibration absorber based on a designable quasi-zero stiffness beam

Xinyu Lian [a], Huaxia Deng [b,*], Guanghui Han [a], Fan Jiang [c,*], Lei Zhu [c], Mingdong Shao [c], Xintong Liu [d], Rongchang Hu [a], Yuexiao Gao [a], Mengchao Ma [a], Xiang Zhong [a]

[a] School of Instrument Science and Opto-electronics Engineering, Hefei University of Technology, Hefei 230009, PR China
[b] CAS Key Laboratory of Mechanical Behavior and Design of Materials, Department of Modern Mechanics, University of Science and Technology of China, Hefei 230027, PR China
[c] Changchun Institute of Optics, Fine Mechanics and Physics, Chinese Academy of Sciences, Changchun 130033, PR China
[d] Technical Institute of Physics and Chemistry, Chinese Academy of Sciences, Beijing 100190, PR China

ARTICLE INFO

Article history:
Received 5 July 2022
Received in revised form 9 October 2022
Accepted 25 November 2022
Available online 1 December 2022
Communicated by Pinqi Xia

Keywords:
Micro vibration
Low frequency
Nonlinear stiffness
Vibration absorber
Passive control
Multi-direction

ABSTRACT

This paper presents a low-frequency micro-vibration absorber based on a beam with designable nonlinear stiffness. The material and dimension parameters of the nonlinear characteristics of the beam are discussed by the finite element method (FEM). Based on the nonlinear stiffness characteristics of the beam, the designed micro-vibration absorber has a low-frequency vibration absorption effect and multiple working modes in multiple directions. The effects of structural parameters on the stiffness characteristics of the designed beam are discussed to explore the low-frequency performance. The results of FEM analysis are verified by vibration absorption experiments, and the effectiveness of the low-frequency vibration absorbers is verified by aerospace micro-vibration experiments.

1. Introduction

With the increasing precision and stability requirements of instruments such as high-resolution cameras, airborne micro-vibration reduction has gradually become a research focus [1–4]. The micro-vibration signals with a small amplitude generated by various equipment components exist in the working environment of precision instruments [5–10], which can last for a long time and constantly deteriorate the operating environment of airborne devices due to the very low ambient damping [11–13]. The vibration signals generated by these devices such as the Stirling chiller contain many low-frequency signals [14], which are difficult to control by traditional passive vibration isolation methods [15–20]. It is still a challenge for airborne low-frequency micro-vibration control [21].

The low-frequency micro-vibration signals are difficult to be measured and evaluated during the spaceborne equipment design process, resulting in the limited installation position of vibration reduction equipment after the completion of the whole equipment. The aviation working environment also puts strict requirements on vibration reduction components' volume, mass, material, and reliability [22–24]. The dynamic vibration absorber (DVA) as a passive vibration control method is concerned, which can attach to the main vibration generating system as a subsystem [25,26]. Frahm developed a passive DVA that can provide complete vibration absorption at operating frequencies [27]. Den Hartog et al. proposed adding damping into the DVA, which can appropriately broaden the frequency band of vibration suppression [28]. XU et al. proposed the concept of Multiple Tuned Mass Dampers (MTMD), which can achieve a better vibration absorption effect and has better robustness [29,30]. Nayfeh et al. propose the multi-degree-of-freedom vibration absorber, which can achieve vibration suppression of multiple modes [31–34]. In recent years, these DVA designs are widely used in ships, buildings, vehicles, railways, etc., and play an important role in practical engineering applications [35,36]. While the vibration magnitude in the traditional field is larger than in precision engineering, the structure and mass of these existing DVAs are correspondingly too large for low-frequency micro-vibration in aviation. The special engineering problem of low-frequency micro-vibration in aviation is eager for a kind of vibration absorber with a simple structure, which can meet

* Corresponding authors.
E-mail address: hxdeng@ustc.edu.cn (H. Deng).

https://doi.org/10.1016/j.ast.2022.108044
1270-9638/

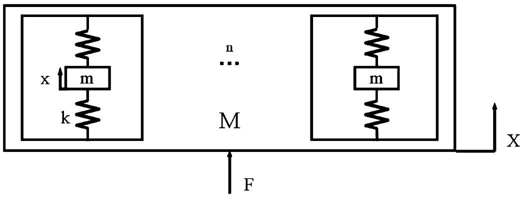

Fig. 1. The simplified equivalent model of the Stirling cryocooler with vibration absorbers.

the working requirements of low-frequency under the requirement of small effective mass.

The vibration absorber is mainly composed of mass components and elastic components. To match the low-frequency vibration absorption requirements with limited mass, it is necessary to propose an elastic element with low stiffness and good structural stability [37–39]. Cai et al. propose a quasi-zero-stiffness metamaterial design and simulated the formation mechanism of ultra-low bandgap through the FEM [40]. Lin et al. propose a new metamaterial of dynamic vibration absorber composed of negative stiffness element to achieve ultra-low bandgap [38]. Lin et al. designed an absorber by combining the negative stiffness and positive stiffness element, which works at 45 Hz. But the effect is not obvious in the interval of negative stiffness and the equipment has a large volume [41]. Nonlinear devices present a new possibility for passive control of low-frequency vibration [42,43] and have been applied in the fields of vibration isolation and shock resistance [44,45]. Optimizing the design of nonlinear devices is important for low-frequency vibration control [46–49].

This paper designs a nonlinear stiffness beam as the elastic element of the vibration absorber to meet the installation space requirements in the aviation environment. Through the optimization of finite element parameters, the stiffness of the beam can be freely designed from negative stiffness to arbitrary stiffness. Which has the characteristics of high static and low dynamic stiffness, theoretically can achieve ultra-low frequency vibration absorption effect. The influence of parameters on nonlinear properties is discussed through FEM, which provides guidance for the design of the micro-vibration absorber. The vibration absorber has a low-frequency micro-vibration absorption capacity. The multiple working modes can absorb multi-frequency vibration energy. The correctness of the simulation results and the effectiveness of low-frequency vibration control are verified by space micro-vibration experiments. The second part of this paper introduces the working principle of the vibration absorber. In the third and fourth parts, the designed curved beam and low-frequency vibration absorber are designed by FEM and the parameters are discussed. The fifth part introduces the vibration absorption experiment of the simply supported beam and the micro-vibration experiment of the aviation Stirling cryocooler.

2. Theoretical analysis

The simplified equivalent model of the Stirling cryocooler with vibration absorbers is shown in Fig. 1. The equivalent mass of the Stirling cryocooler is M, and the equivalent mass of the vibration absorbers is m. X is the vibration displacement of the Stirling cryocooler, x is the equivalent mass displacement of each vibration absorber, k is the equivalent stiffness of the vibration absorber, n is the number of vibration absorbers, and F is the external force acting on the Stirling cryocooler.

Simultaneous equations of motion:

$$\begin{cases} 2k[X(t)-x(t)] = m\ddot{x}(t) \\ F(t) = M\ddot{X}(t) + 2nk[X(t)-x(t)] \end{cases} \tag{1}$$

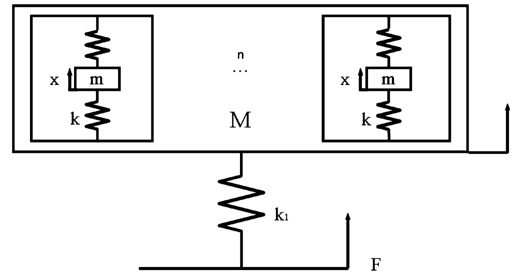

Fig. 2. The model of the system when disturbed by external forces.

Laplace transform:

$$\begin{cases} 2k[X(s)-x(s)] = ms^2x(s) \\ F(s) = Ms^2X(s) + 2nk[X(s)-x(s)] \end{cases} \tag{2}$$

$$X(s) = \left(\frac{m}{2k}s^2+1\right)x(s) \tag{3}$$

The transfer function is available:

$$\frac{x(s)}{X(s)} = \frac{m}{2k}s^2+1 \tag{4}$$

$$\frac{x(s)}{X(s)} = \frac{2k}{2k-m\omega^2} \tag{5}$$

The momentum theorem:

$$nm\dot{x}(t) + M\dot{X}(t) = \bar{M}\dot{X}(t) \tag{6}$$

Equivalent mass of the system:

$$\bar{M} = M + \frac{2k*nm}{2k-m\omega^2} \tag{7}$$

When $\sqrt{\frac{2k}{m}} < \omega < \sqrt{\frac{2k}{m}+\frac{2nk}{M}}$, $\bar{M} < 0$

When the system is disturbed by external forces, it can be equivalent to the model shown in Fig. 2. The disturbance F is connected to the whole system through an elastic element with stiffness k_1. The displacement of the system is x_2 and the displacement of the excitation end is x_1.

$$k_1\,(x_1-x_2) = \bar{M}\ddot{x}_2 \tag{8}$$

$$\bar{M} = M + \frac{2k*nm}{2k-m\omega^2} \tag{9}$$

The vibration transmissibility is:

$$\frac{x_2}{x_1} = \frac{k_1\left(2k-m\omega^2\right)}{mM\omega^4-(mk_1+2kM+2nmk)\,\omega^2+2kk_1} \tag{10}$$

The transfer curve in Fig. 3 can be obtained from the transfer function Eq. (10), and the asymptotes are shown in Eq. (11) and Eq. (12), where $\tau = m*n$, $\varphi = m*M$.

$$x_1 = \frac{\sqrt{2}\sqrt{\varphi\left(2(\tau+M)+m+\sqrt{4(\tau^2+2M\tau+m\tau+M^2-\varphi)+m^2}\right)k}}{2\varphi} \tag{11}$$

$$x_2 = \frac{\sqrt{2}\sqrt{\varphi\left(2(\tau+M)+m-\sqrt{4(\tau^2+2M\tau+m\tau+M^2-\varphi)+m^2}\right)k}}{2\varphi} \tag{12}$$

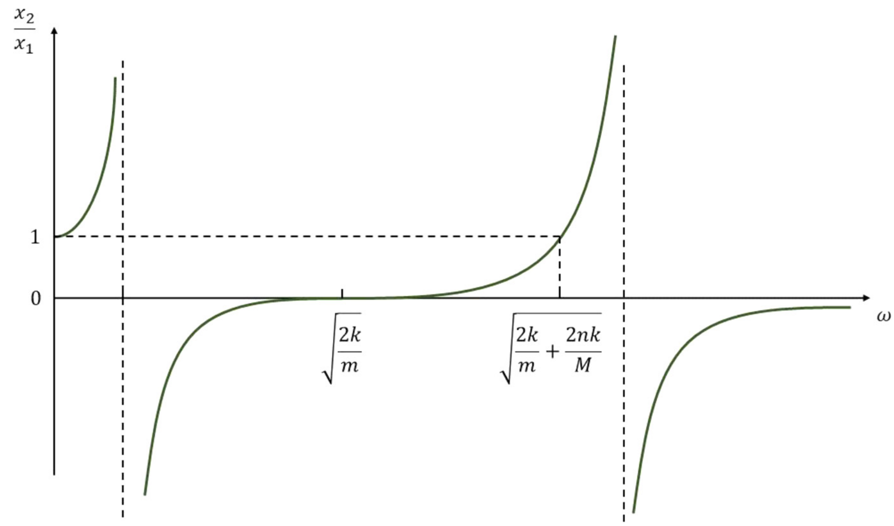

Fig. 3. The transfer curve.

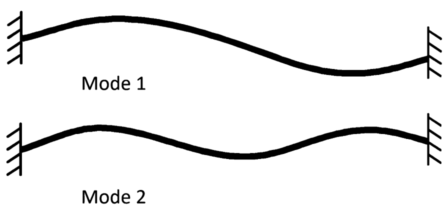

Fig. 4. Buckling modes for the beam.

When the whole system is in the equivalent negative mass condition, that is, the frequency of the disturbance signal ω is: $\sqrt{\frac{2k}{m}} < \omega < \sqrt{\frac{2k}{m} + \frac{2nk}{M}}$, the vibration can be attenuated effectively. Similar local resonance structures are also known as vibration absorbers, which can effectively suppress the vibration of the system at a specific frequency. At the same time, increasing the number of vibration absorbers (increase the value of n) can increase the frequency range of vibration reduction and improve the vibration absorption effect.

3. Design of nonlinear stiffness beam

The effect of the vibration absorber depends on the natural frequency of a single vibration absorber. When the natural frequency of the vibration absorber is equal to the frequency of the disturbing signal, the resonance structure can absorb the energy to the greatest extent and achieve the best damping effect. The key problem in designing a vibration absorber is to design the natural frequency. The natural frequency of the vibration absorber is related to the quality and stiffness of the structure. The low-frequency micro-vibration problem in aerospace often appears in the stage after the structural design of the whole machine. At this time, the installation position and space are limited. The material, size, quality, and other aspects of the vibration absorber are subjected to many restrictions. To control the overall quality of the vibration absorber and achieve low-frequency vibration absorption, a special curved beam is designed as the elastic support element of the vibration absorber. This kind of curved beam has nonlinear stiffness, can achieve high static stiffness and low dynamic stiffness, and has a negative stiffness working interval, theoretically can meet ultra-low frequency vibration absorber design.

When restricting lateral movement at both ends of the beam. The boundary conditions are shown in Eq. (13), where w is the lateral beam displacement, l is the length of the curved beam.

$$w(0) = w(l) = 0, \quad \left(\frac{dw}{dx}\right)_{x=0} = \left(\frac{dw}{dx}\right)_{x=l} = 0 \tag{13}$$

The buckling modes for the beam are shown in Fig. 4. When one end of the beam is subjected to a vertical force, the stiffness of the beam decreases during the transition from mode 1 to mode 2, which is related to the shape and the material.

To discuss the influence of curvature on stiffness, beams with three kinds of curvature in Fig. 5 are designed through five control points. The coordinates of vertices A and B at both ends are (0,0) and (20,10) respectively. The bending of beam I to beam III gradually increases. When the fixed constraint is applied to point A of the beam and the vertical downward force is applied to point B, the nonlinear mechanical properties of the beam can be obtained. Fig. 6 (a) is the stress of the beam after deformation. Fig. 6 (b) is the force curve of different beams when changing displacement and Fig. 6 (c) is the stiffness character. By observing the mechanical properties, it can be found that the designed beam has the characteristics of high static stiffness and low dynamic stiffness. With the curvature decreasing of the beam, the stiffness can gradually achieve quasi-zero stiffness or even negative stiffness.

When the thickness of the beam is changed, the stiffness characteristics are shown in Fig. 6 (d). When the beam thickness is doubled, the dynamic stiffness will be increased by about eight times and the static stiffness by about six times. The parametrically designed beam has strong nonlinear stiffness editing ability within limits.

To analyze the influence of materials on the stiffness of beams, the mechanical properties of rubber and iron beams are discussed. The Young's modulus of rubber is 3.6 MPa, Poisson's ratio is 0.49, and density is 1300 Kg/m^3. The results are shown in Fig. 6 (e). For this designed beam, rubber with higher elasticity can be used to design higher stiffness, when the structural design parameters remain unchanged, and the beam thickness is thin. Beams of different materials can achieve the effect of editing stiffness through shape design. Therefore, the main consideration in material selection is structural stability.

4. Design of micro-vibration absorber

Fig. 7 shows the model of the vibration absorber and the actual vibration absorber. The vibration absorber comprises three parts: installation module, elastic module and mass module. The installation module is at the bottom of the vibration absorber and is designed with an arc shape. The installation module can fit the

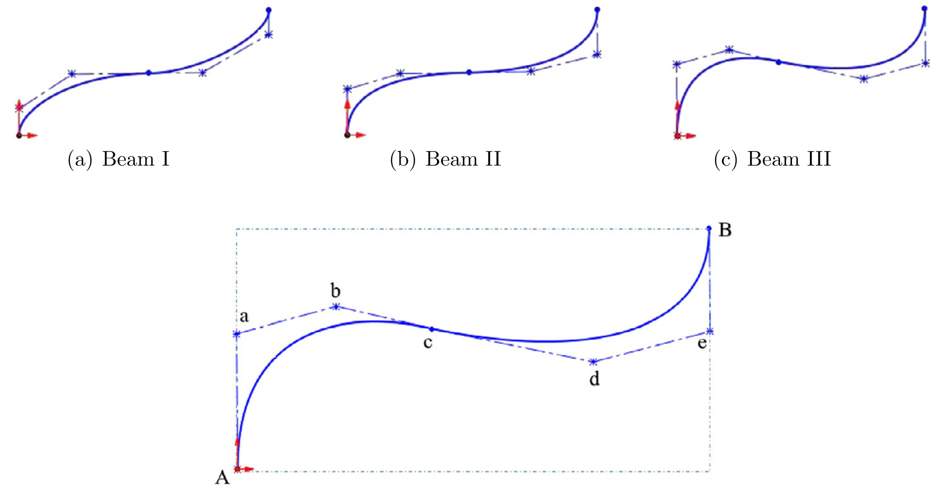

(a) Beam I (b) Beam II (c) Beam III

(d) The curvature control point

Fig. 5. Three kinds of beam.

curved mounting surface on the Stirling chiller and can be conveniently installed in the critical position of the vibration equipment by pasting. The vibration energy can be transferred to the absorber to realize energy transfer. Above the installation module is the elastic module. To ensure the stability of the vibration absorber, the elastic module is composed of two symmetric curved beams. As the middle module of the vibration absorber, both ends of the curved beam need to be tightly fixed on the quality module and the installation module to ensure the working effect. The designed beam and the installation module are uniformly processed with rubber material and the bond plane with the upper mass block is reserved. On the top of the vibration absorber is the mass module, which can adjust the working range of the vibration absorber by changing the mass according to different requirements in actual use. The material used in the rubber beam structure meets the requirements of aviation standards and has lower stiffness after finite element simulation. The overall vibration absorber size is 12 mm*12 mm*52 mm, which meets the requirements of installation and weight for aerospace. The whole structure is simulated by the FEM to optimize design parameters. The influence of parameters on the natural frequency of the vibration absorber is discussed below.

The force diagram of the low-frequency vibration absorber composed of the beam with adjustable stiffness is shown in Fig. 8. This structure can transfer vibration step by step from the bottom vibration source to the upper mass module to complete the energy transfer, which can reduce the vibration of the main equipment.

The vibration absorber base on this structure not only has a low natural frequency but also has the ability of vibration absorption in multiple directions. In Fig. 9, the stiffness varies with displacement in three different directions. The vibration absorber in the X and Z directions has the properties of high static stiffness and low dynamic stiffness. The stiffness in the Y direction increases with the increase of displacement. It is found that the absorber has small stiffness in the Y and Z directions. The stiffness of the three directions varies little in a small displacement interval, so a stable vibration absorption frequency can be obtained during working.

The vibration absorber is fixed on a curved vibrating rigid body to observe the dynamic response. The simulation was carried out by changing the direction of the vibration signal, and the signal amplitude was 0.5 N, as shown in Fig. 10. Fig. 11 (a) shows the dynamic response of applying force excitation in three directions. The Y and Z directions with lower stiffness of the absorber have lower natural frequencies than the X direction. When the vibration absorber is excited in three directions, the dynamic response is the superposition of the response in the other three directions. Indicating that the vibration absorber can work in multiple directions and can absorb the vibration of multiple frequencies.

The working frequency of the vibration absorber can be designed by adjusting the stiffness and mass. In Fig. 11 (b) and (c), the frequency domain response of the vibration absorber is shown by applying excitation in three directions after changing the mass. As the mass increases, the natural frequencies in all three directions of the system decrease.

5. Experiments

5.1. Vibration absorption experiment of the simply supported beam

The vibration absorption experiment of the simply supported beam is designed to verify the vibration absorption effect of low-frequency vibration absorbers. As shown in Fig. 12. As the vibration source of the experiment, the simply supported beam is fixed on the bracket at both ends and connected to the vibration exciter by double-headed screws. The type of vibration exciter is DH40020. An acceleration sensor is fixed on the beam to measure the dynamic response. The acceleration sensor type is DH1A102E, and the sensitivity is 1.11 mv/m/s^2. The surface bonded to the beam is used to install the vibration absorber module. A small acceleration sensor measures the vibration response signal of the vibration absorber at the upper end. The frequency response function of the vibration absorber is calculated to observe the vibration absorption effect. The type of the small acceleration sensor is DH132, and the sensitivity is 1.663 pc/g. The charge adaptor type of the small sensor is DH5857-1. The vibration excitation controller can change the signal output mode and power of the vibration exciter. The type of vibration excitation controller is DH1301. In this experiment, the input of the simply supported beam is set to a sweep frequency signal of 10-300 Hz, and the power is 160 W. The acceleration acquisition system type is DH5922, which can collect the signal of multiple acceleration sensors. The controller for the acceleration acquisition system can display and save these signals. By comparing the beam's acceleration under unified vibration excitation before and after the vibration absorber's installation, the control effect of the absorber on the vibration can be obtained.

The dynamic response of the beam without vibration absorbers under the excitation of a 10-300 Hz sweep signal is shown in Fig. 13. The beam has a fourth-order resonance when the frequency is less than 300 Hz, and the first-order resonance peak is about 39 Hz.

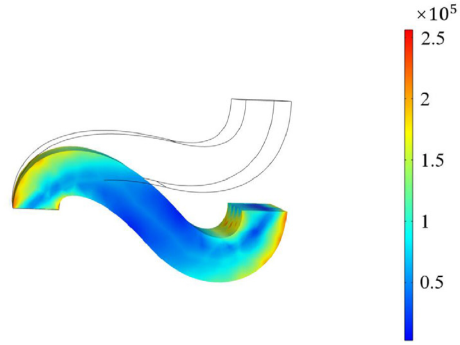

(a) Stress deformation condition

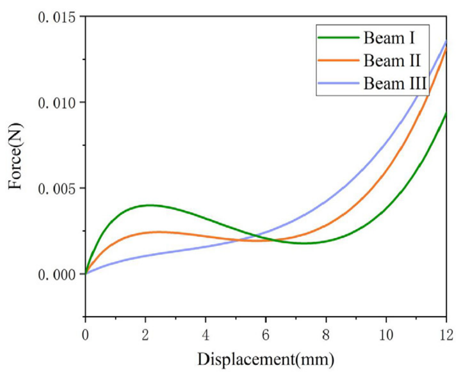

(b) F of different beams

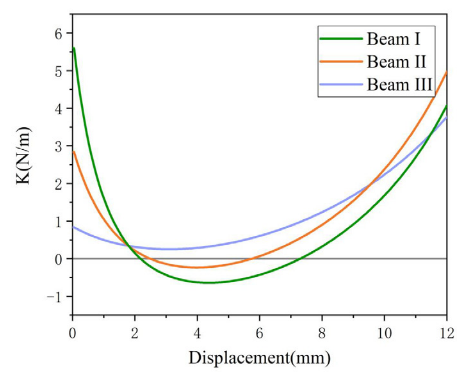

(c) K of different beams

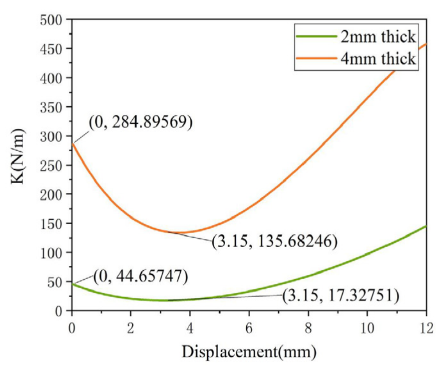

(d) Change the thick of beams

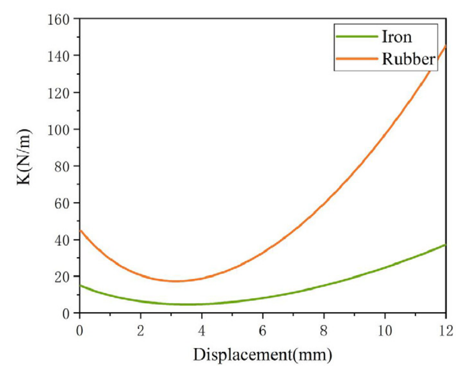

(e) Change the material

Fig. 6. Nonlinear mechanical properties of different beams. (For interpretation of the colors in the figure(s), the reader is referred to the web version of this article.)

(a) The model of vibration absorber

(b) The prototype

Fig. 7. The micro-vibration absorbing module.

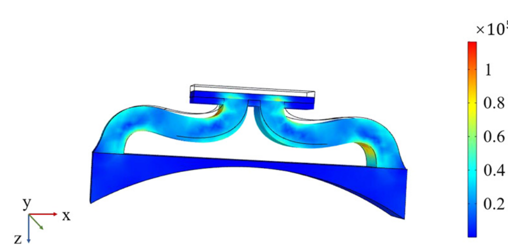

Fig. 8. Low frequency vibration absorber working force diagram.

To reduce the vibration of the beam at the first natural frequency, a vibration absorber with an appropriate frequency should be selected. The natural frequency of the vibration absorber can be calculated by changing the mass module and measuring the dynamic response curve of the vibration absorber. The comparison of natural frequency experimental results and simulation results is shown in Fig. 14. The natural frequency of the vibration absorber decreases with the increase of the mass. Adjusting the mass, a vibration absorber with a natural frequency of 39 Hz can be obtained. Three dynamic vibration absorbers are selected as shown in Fig. 15. The natural frequency of module I and module II is 41.5 Hz, and module III is 37 Hz. Fig. 16 shows the comparison of the

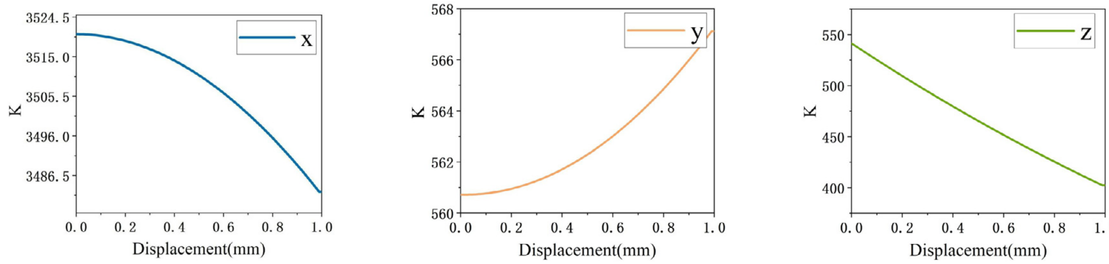

(a) Stiffness of x direction (b) Stiffness of y direction (c) Stiffness of z direction

Fig. 9. Stiffness of vibration absorber in three directions.

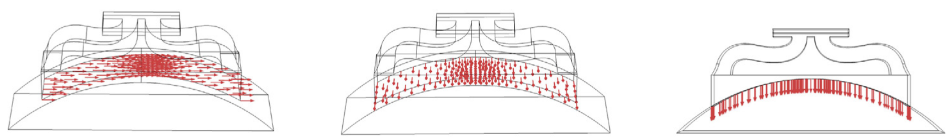

(a) The x direction (b) The y direction (c) The z direction

Fig. 10. Schematic diagram of excitation.

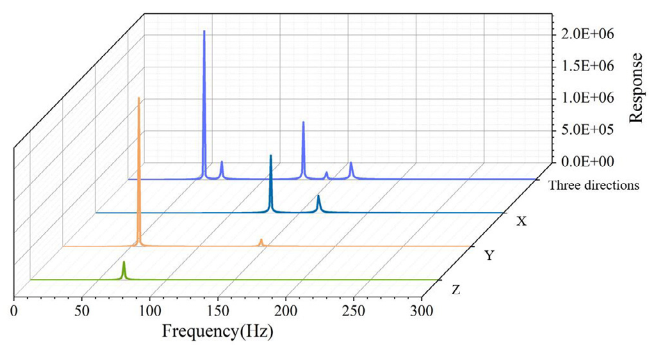

(a) Response diagram of different direction excitation

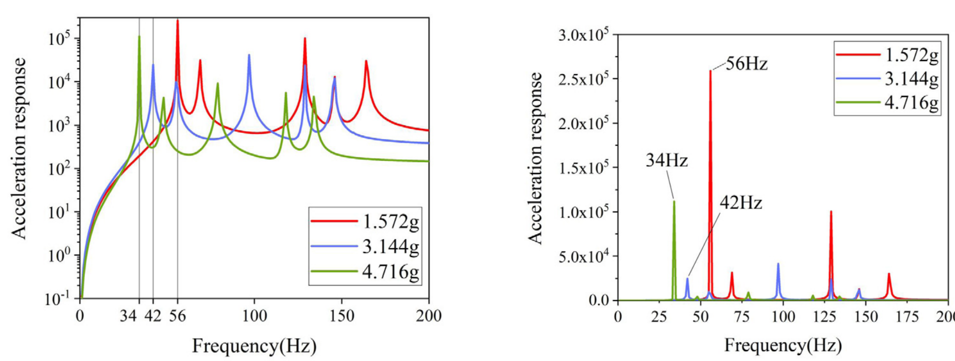

(b) Frequency domain response diagram for changing mass (c) Frequency domain response diagram for changing mass

Fig. 11. Nonlinear mechanical properties of vibration absorber.

response signal in the time domain between the simply supported beam and the beam with vibration absorbers under the input of 10-300 Hz sweep signal.

The vibration absorption experiment includes:

1. Testing the vibration absorption effect of multiple vibration absorbers with the same natural frequency.

2. Testing the vibration absorption effect of multiple vibration absorbers with different natural frequencies.

In Fig. 16 (a), the dark purple curve is the response of the beam after installing one vibration absorber with the natural frequency of 41 Hz, and the light purple curve is the response of the beam with two vibration absorbers with the same 41 Hz frequency. The installation of a vibration absorber with an appropriate natural frequency has a significant effect on the vibration decrease of beams. Multiple vibration absorbers with the same natural frequency can enlarge the frequency range of vibration re-

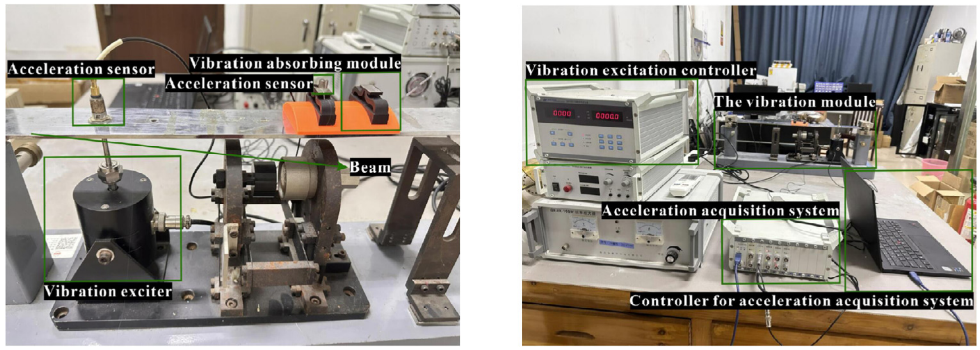

(a) The vibration module (b) The control module

Fig. 12. The vibration absorption experiment.

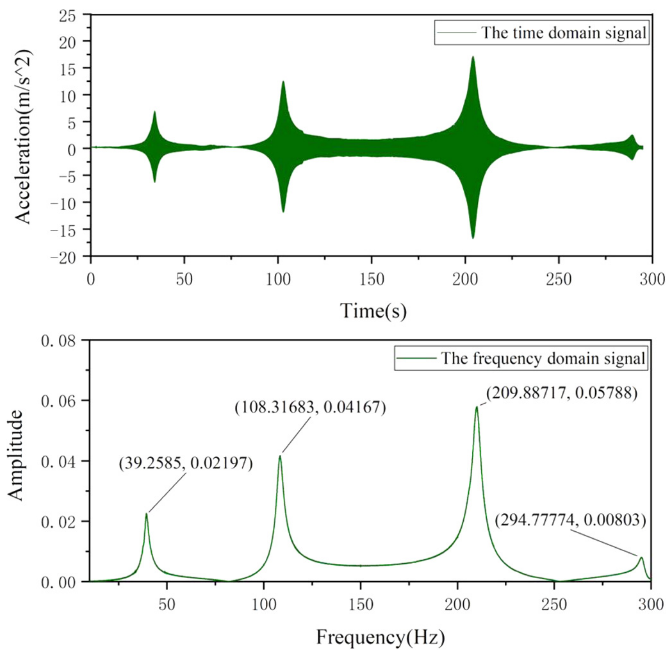

Fig. 13. The dynamic response of the simply supported beam.

duction and increase the efficiency of vibration reduction at the center frequency. In Fig. 16 (b), the light violet curve is the response of the beam installed with two vibration absorbers with the frequency of 41 Hz, and the orange curve is the response installed with two vibration absorbers with 41 Hz and one vibration absorber with 37 Hz. When installing three modules, the absorption of the vibration reduction is improved efficiently. The vibration absorbers with different natural frequencies are coupled with each other. Each vibration absorber acts independently at its own natural frequency which can broaden the frequency band of vibration absorption. The coupling effect between modules can further form a vibration pass band and gap band by artificial design.

Fig. 17 is the comparison of beam response in the frequency domain with multiple vibration absorbers. The response in the frequency domain can be further seen that when a single vibration absorber is added, the vibration amplitude at natural frequency is reduced by about 88% and the peak value is reduced by 55.43%. When two vibration absorbers with the same frequency are added, the vibration decreases by 93% and increases by 5% compared with one absorber, and the frequency band of vibration reduction expands by 48%. When three vibration absorbers of different frequencies are added, the frequency band of vibration reduction is further widened, and the vibration peak value is reduced by about 68%. The working efficiency of the vibration absorber is related to the number and natural frequency of the vibration absorber installed, as well as the vibration energy generated by the installation position. However, the scientific design of vibration absorber array arrangement can realize low-frequency vibration reduction in a wide band.

5.2. Stirling cryocooler vibration absorption experiment

The vibration test equipment of the aviation Stirling cryocooler is shown in Fig. 18. The vibration signal of the Stirling cryocooler is collected by acceleration sensors and the multi-component dynamometer. Two computers control the micro-force acquisition system and acceleration acquisition system respectively. Below the Stirling cryocooler is the multi-component dynamometer of KISTLER and the type is 9255 C. Its high resolution enables the smallest dynamic changes in large forces to be measured. The dynamometer consists of four 3-component force sensors fitted under high preload between a base plate and a top plate. The measurement resolution is less than 0.01 N.

Fig. 19 (a) is the overall structure of the Stirling cryocooler, which is divided into two parts: the compressor and the cold finger. Both parts are connected by pipe bending. One end of the compressor is equipped with a triaxial accelerometer, and one acceleration sensor is installed at the cold finger to measure and analyze the acceleration signal of the vibration source. The Stirling cryocooler is working under a 50 Hz-55 Hz excitation signal, which affects the effect of the chiller. During the working process, the compressor and pipe are the main vibration source of the micro-vibration problem. Through the analysis of the frequency domain of the collected signals, the generated vibration signals mainly focus on the input signal frequency and its frequency doubling.

The acceleration of the compressor and cold finger under 50 Hz and 54 Hz excitation is shown in Fig. 20. The vibration isolators around the compressor can limit the vibration of the compressor to a certain extent. The vibration magnitude of the compressor is smaller than that of the cold finger. The peak-to-peak value of the vibration acceleration is less than 1 m/s^2. The vibration in the y-direction of the compressor is weak. By measuring the vibration acceleration in the y-direction of the upper end of the cold finger as shown in Fig. 20 (c), it can be determined that the vibration in this direction is mainly generated at the pipe bending. When the excitation frequency of the Stirling cryocooler is changed, the amplitude of the vibration signal also changes. Fig. 20 (c) shows that the amplitude

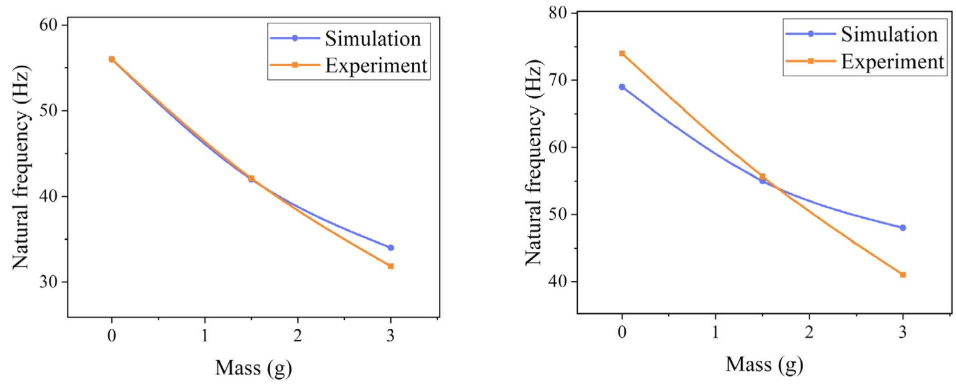

(a) Natural frequency of y direction

(b) Natural frequency of z direction

Fig. 14. Natural frequency of vibration absorber.

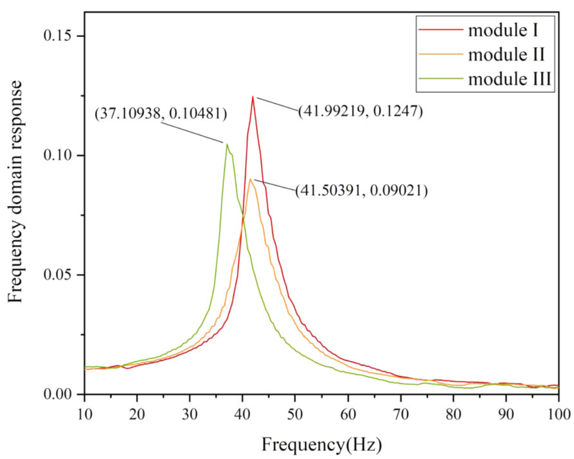

Fig. 15. The frequency domain response of vibration absorbers.

Table 1
The micro force of the Stirling cryocooler.

Direcrion	x	y	z
Compressor	0.187 N	0.118 N	0.0214 N
Cold finger	0.082 N	0.14 N	0.189 N

Table 2
The micro force of Stirling cryocooler with vibration absorbers.

Direcrion	x	y	z
Compressor	0.204 N	0.0035 N	0.0247 N
Cold finger	0.0724 N	0.0954 N	0.0616 N

of vibration acceleration generated by pipe bending at 50 Hz is greater than 54 Hz. The peak-to-peak value of 50 Hz is about 1.4 m/s^2.

Fig. 21 shows the frequency domain analysis of the acceleration signal when the excitation frequency is changed. The vibration signal generated by the Stirling cryocooler is related to the excitation signal frequency. The energy is mainly concentrated in the excitation signal frequency and its frequency doubling, and the signal component on the fundamental frequency is the largest when excitation is 50 Hz.

It can be concluded that the main vibration frequency is also changed when changing the excitation. While the refrigeration effect of the refrigerator is better under the 50 Hz excitation than 54 Hz, the actual power is about 50 W during working. Therefore, in the case of 50 W input power and 50 Hz input signal, a vibration absorber is installed for testing. After vibration signal analysis, install the vibration absorber at the connecting pipe, as shown in Fig. 19 (b).

In the passive state, the micro force of the Stirling cryocooler measured by the Multi-Component Dynamometer at 50 Hz is shown in Table 1. Table 2 is the force of the Stirling cryocooler with vibration absorbers. The difference between the data in Table 1 and Table 2 shows that the vibration of the compressor in the y-direction is obviously weakened after the connecting pipe is installed with vibration absorbers. The micro-force decreased by 97%, from 0.118 N to 0.0035 N. The measured micro-forces in the three directions of the cold finger all decreased, from 0.082 N to 0.0724 N in the x-direction, from 0.14 N to 0.0954 N in the y-direction, and from 0.189 N to 0.0616 N in the z-direction.

The curves in Fig. 22 are the acceleration signals measured by the acceleration sensor installed at the top of the cold finger. The green and yellow curves are the contrast signals before and after the installation of the vibration absorbers. The time-domain signal is processed by 10-300 Hz band-pass filtering to filter out the interference to the experiment in the environment. The amplitude of acceleration decreases by 50% after vibration absorption in the full frequency band of 10-300 Hz. The vibration absorber acts on the 50 Hz fundamental frequency signal, and the vibration absorption efficiency can reach 68.364%. The force in three directions of the cold finger during vibration is less than 0.1 N by the micro force test with the aeronautical micro-vibration absorber. The installation of absorbers at the pipe can significantly reduce the vibration of the compressor in the Y direction, which is most disturbed by the pipe vibration. Make the vibration micro-force of the equipment meet the requirements of the aviation index.

The above experimental results prove that the vibration absorber can control the low-frequency micro-vibration generated by precision instruments. As a subsystem attached to the main vibration system, it can meet the requirements of materials and installation space in precision experiments. By adjusting the structure parameters of the vibration absorber, the vibration reduction of linear spectrum signals with different frequencies can be realized, which has flexibility in practical application. The vibration absorber belongs to the passive vibration control method and has stability in aerospace and other fields.

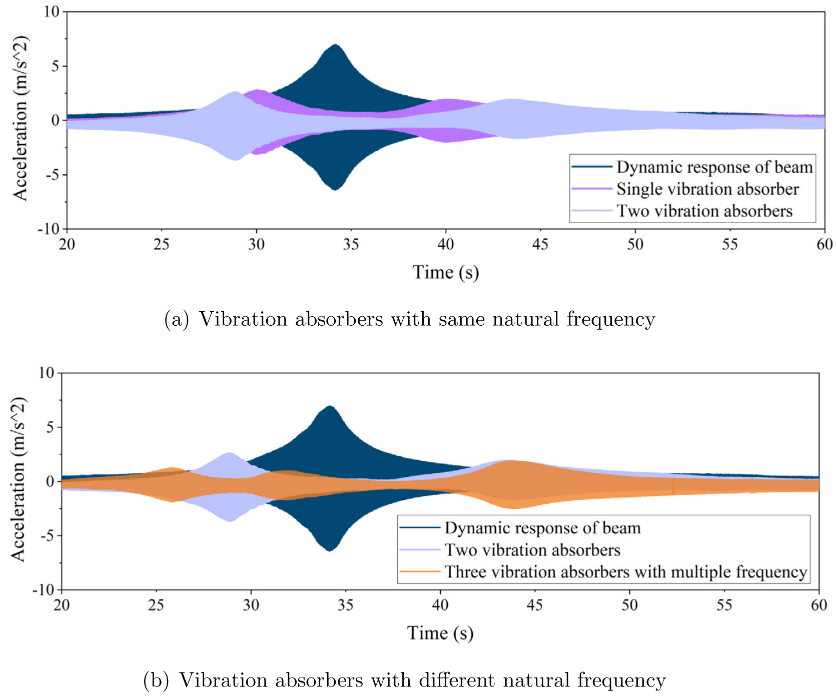

Fig. 16. Vibration absorption experiments.

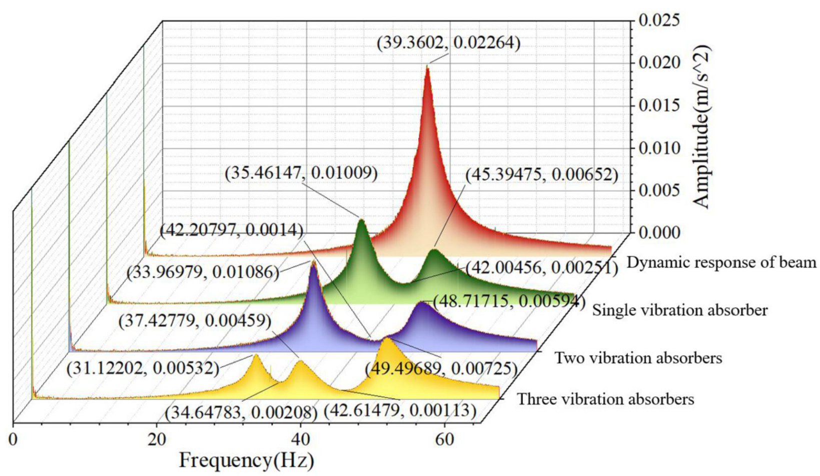

Fig. 17. Vibration absorption experiments in frequency domain.

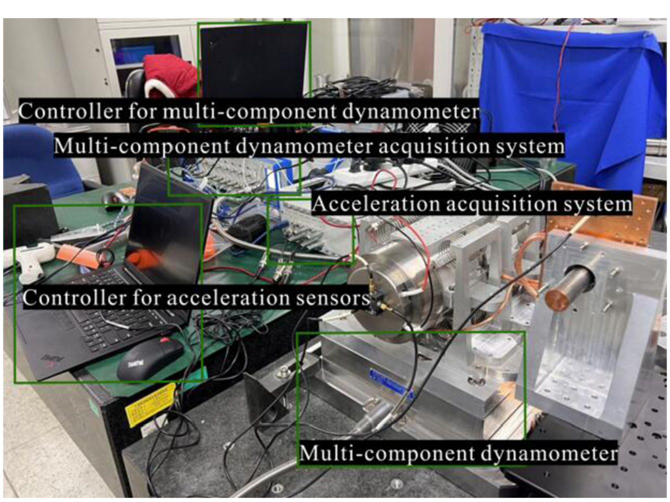

Fig. 18. The equipment of the Stirling cryocooler vibration absorption experiment.

6. Conclusions

In this paper, a vibration absorber for low-frequency micro-vibration in aviation is developed based on a designable nonlinear stiffness beam. The results show that through parameter adjustment of the beam can obtain ideal quasi zero stiffness and negative stiffness characteristics and implement free adjustable stiffness of low-frequency vibration absorber. The designed vibration absorber significantly reduces the size and mass of the structure and improves the working stability. The experimental results show that the vibration in the working direction can be reduced by about 97% and the total power in the full frequency domain can be reduced by about 50% after installing the vibration absorber. The proposed vibration absorber has a potential application in the field of micro-vibration control of aerospace loads and provides a new idea for realizing low-frequency multi-directional vibration control of components with nonlinear characteristics.

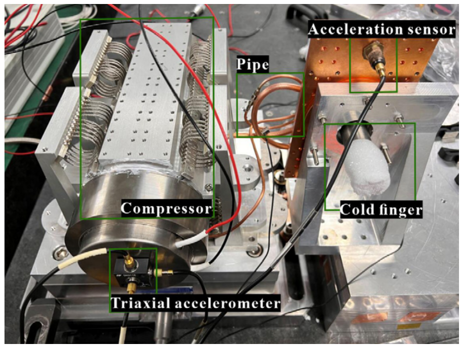

(a) The stirling cryocooler

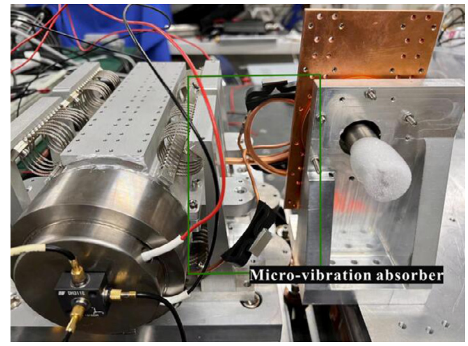

(b) The stirling cryocooler with absorbers

Fig. 19. The Stirling cryocooler structure.

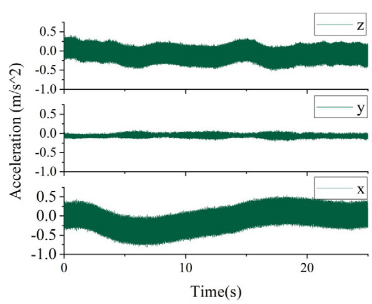

(a) The acceleration in three directions under 50Hz excitation

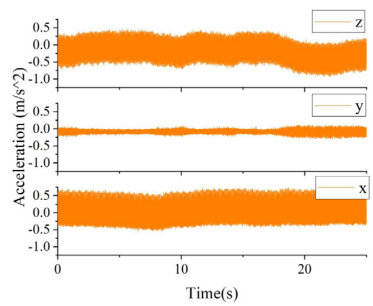

(b) The acceleration in three directions under 54Hz excitation

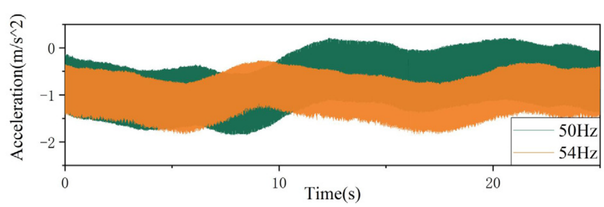

(c) Acceleration of the cold finger

Fig. 20. The time-domain signal (X is the direction of the pipe, Y is the direction of the cold finger, and Z is the vertical direction.)

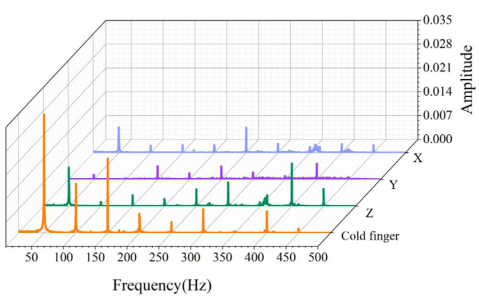

(a) 50Hz

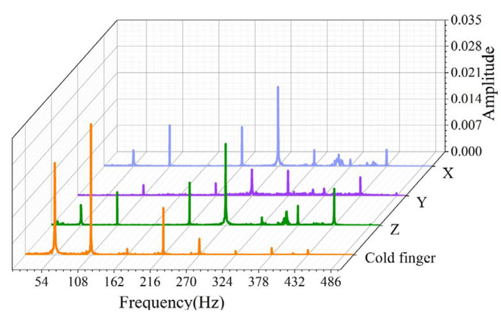

(b) 54Hz

Fig. 21. The frequency-domain signal (X is the direction of the pipe, Y is the direction of the cold finger, and Z is the vertical direction.)

Publishing ethics statement

This manuscript strictly complies with the ethical code of the World Medical Association. The research work does not involve human experiments and animal experiments, and meets the unified submission requirements of journal.

Declaration of competing interest

The authors declare that they have no known competing financial interests or personal relationships that could have appeared to influence the work reported in this paper.

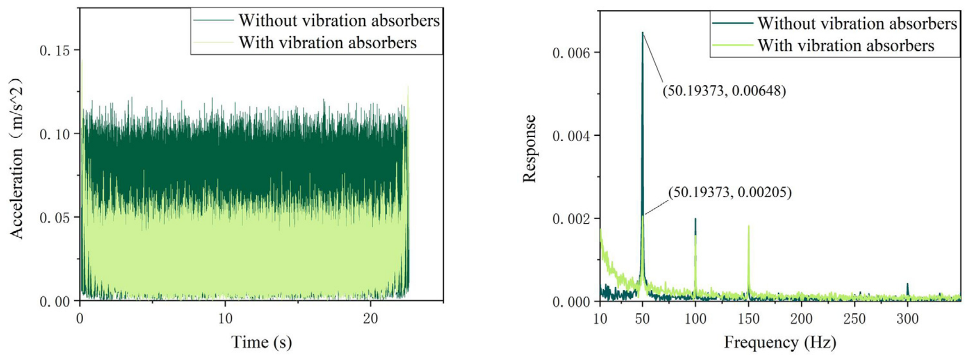

(a) Time-domain acceleration

(b) Frequency-domain response

Fig. 22. Acceleration of the cold finger.

Data availability

The data that has been used is confidential.

Acknowledgement

This work is supported by National Natural Science Foundation of China (Grant Nos. 11872167 and 52275529) and Natural Science Foundation of Anhui Province(1908085J15).

References

[1] S. Chen, M. Xuan, J. Xin, Y. Liu, S. Gu, J. Li, L. Zhang, Design and experiment of dual micro-vibration isolation system for optical satellite flywheel, Int. J. Mech. Sci. 179 (2020) 105592, https://doi.org/10.1016/j.ijmecsci.2020.105592.
[2] R. Yue, H. Wang, T. Jin, Y. Gao, X. Sun, T. Yan, J. Zang, K. Yin, S. Wang, Image motion measurement and image restoration system based on an inertial reference laser, Sensors 21 (2021) 3309, https://doi.org/10.3390/s21103309.
[3] T. Deng, G. Wen, H. Ding, Z.-Q. Lu, L.-Q. Chen, A bio-inspired isolator based on characteristics of quasi-zero stiffness and bird multi-layer neck, Mech. Syst. Signal Process. 145 (2020) 106967, https://doi.org/10.1016/j.ymssp.2020.106967.
[4] M. Wang, Y. Hu, Y. Sun, J. Ding, H. Pu, S. Yuan, J. Zhao, Y. Peng, S. Xie, J. Luo, An adjustable low-frequency vibration isolation Stewart platform based on electromagnetic negative stiffness, Int. J. Mech. Sci. 181 (2020) 105714, https://doi.org/10.1016/j.ijmecsci.2020.105714, https://www.sciencedirect.com/science/article/pii/S0020740319336756.
[5] T. Wacker, L. Weimer, K. Eckert, GOCE platform micro-vibration verification by test and analysis, in: Proceedings of the European Conference on Spacecraft Structures, Materials and Mechanical Testing, 2005, pp. 10–12.
[6] A. Preumont, M. Horodinca, I. Romanescu, B. de Marneffe, M. Avraam, A. Deraemaeker, F. Bossens, A. Abu Hanieh, A six-axis single-stage active vibration isolator based on Stewart platform, J. Sound Vib. 300 (3) (2007) 644–661, https://doi.org/10.1016/j.jsv.2006.07.050, https://www.sciencedirect.com/science/article/pii/S0022460X06007334.
[7] X. Jiao, Y. Zhao, W. Ma, Nonlinear dynamic characteristics of a micro-vibration fluid viscous damper, Nonlinear Dyn. 92 (5) (2018), https://doi.org/10.1007/s11071-018-4116-2.
[8] D. Lim, H. Kim, K. Yee, Uncertainty propagation in flight performance of multirotor with parametric and model uncertainties, Aerosp. Sci. Technol. 122 (2022) 107398, https://doi.org/10.1016/j.ast.2022.107398, https://www.sciencedirect.com/science/article/pii/S1270963822000724.
[9] P. Zhang, S. Firuzi, C. Yuan, X. Gong, S. Gong, General passive stability criteria for a sun-pointing attitude using the metasurface sail, Aerosp. Sci. Technol. 122 (2022) 107380, https://doi.org/10.1016/j.ast.2022.107380, https://www.sciencedirect.com/science/article/pii/S1270963822000542.
[10] G. Suryanarayana, D. Singh, S. Surya, G. Jagadeesh, Nonlinear damping model for supersonic air-intake buzz, Aerosp. Sci. Technol. 126 (2022) 107567, https://doi.org/10.1016/j.ast.2022.107567, https://www.sciencedirect.com/science/article/pii/S1270963822002413.
[11] D. Kamesh, R. Pandiyan, A. Ghosal, Modeling, design and analysis of low frequency platform for attenuating micro-vibration in spacecraft, J. Sound Vib. 329 (17) (2010) 3431–3450, https://doi.org/10.1016/j.jsv.2010.03.008.
[12] C. Liu, X. Jing, S. Daley, F. Li, Recent advances in micro-vibration isolation, Mech. Syst. Signal Process. 56–57 (2015) 55–80, https://doi.org/10.1016/j.ymssp.2014.10.007, https://www.sciencedirect.com/science/article/pii/S0888327014004014.
[13] B. Wang, Z. Liu, P. Zheng, Rigid-flexible coupling dynamic modeling and analysis of dumbbell-shaped spacecraft, Aerosp. Sci. Technol. 126 (2022) 107641, https://doi.org/10.1016/j.ast.2022.107641, https://www.sciencedirect.com/science/article/pii/S1270963822003157.
[14] P. Xu, T. Liu, S. Pan, Z. Zhou, Numerical analysis for micro-vibration isolation of jointed sandwich plates with mass blocks, Mater. Today Commun. 17 (2018) 341–354, https://doi.org/10.1016/j.mtcomm.2018.09.018, https://www.sciencedirect.com/science/article/pii/S2352492818303295.
[15] A. Stabile, G.S. Aglietti, G. Richardson, G. Smet, A 2-collinear-DoF strut with embedded negative-resistance electromagnetic shunt dampers for spacecraft micro-vibration, Smart Mater. Struct. 26 (4) (2017) 045031, https://doi.org/10.1088/1361-665x/aa61e3.
[16] D. Xu, Q. Yu, J. Zhou, S. Bishop, Theoretical and experimental analyses of a nonlinear magnetic vibration isolator with quasi-zero-stiffness characteristic, J. Sound Vib. 332 (14) (2013) 3377–3389, https://doi.org/10.1016/j.jsv.2013.01.034, https://www.sciencedirect.com/science/article/pii/S0022460X13000849.
[17] X. Sun, B. Yang, L. Zhao, X. Sun, Optimal design and experimental analyses of a new micro-vibration control payload-platform, J. Sound Vib. 374 (2016) 43–60, https://doi.org/10.1016/j.jsv.2016.04.007, https://www.sciencedirect.com/science/article/pii/S0022460X16300414.
[18] G. Aglietti, R. Langley, E. Rogers, S. Gabriel, Model building and verification for active control of microvibrations with probabilistic assessment of the effects of uncertainties, Proc. Inst. Mech. Eng., Part C, J. Mech. Eng. Sci. 218 (4) (2004), https://doi.org/10.1177/095440620421800404.
[19] Z. Zhang, G.S. Aglietti, W. Zhou, Microvibrations induced by a cantilevered wheel assembly with a soft-suspension system, AIAA J. 49 (5) (2011) 1067–1079, https://doi.org/10.2514/1.J050791.
[20] A. Preumont, M. Horodinca, I. Romanescu, B. Marneffe, M. Avraam, A. Deraemaeker, F. Bossens, A. Abu Hanieh, A six-axis single-stage active vibration isolator based on Stewart platform, J. Sound Vib. 300 (2007) 644–661, https://doi.org/10.1016/j.jsv.2006.07.050.
[21] X. Wang, H. Wu, B. Yang, Micro-vibration suppressing using electromagnetic absorber and magnetostrictive isolator combined platform, Mech. Syst. Signal Process. 139 (2020) 106606, https://doi.org/10.1016/j.ymssp.2019.106606, https://www.sciencedirect.com/science/article/pii/S0888327019308271.
[22] T. Sales, D. Rade, L. de Souza, Passive vibration control of flexible spacecraft using shunted piezoelectric transducers, Aerosp. Sci. Technol. 29 (1) (2013) 403–412, https://doi.org/10.1016/j.ast.2013.05.001, https://www.sciencedirect.com/science/article/pii/S127096381300093X.
[23] M.N. Hasan, M. Haris, S. Qin, Flexible spacecraft's active fault-tolerant and anti-unwinding attitude control with vibration suppression, Aerosp. Sci. Technol. 122 (2022) 107397, https://doi.org/10.1016/j.ast.2022.107397, https://www.sciencedirect.com/science/article/pii/S1270963822000712.
[24] W. Wu, J. Zhao, J. Zhong, Influence of the rotating direction and speed of controllable speed casing on the flow stability of a transonic compressor rotor under design condition, Aerosp. Sci. Technol. 126 (2022) 107630, https://doi.org/10.1016/j.ast.2022.107630, https://www.sciencedirect.com/science/article/pii/S1270963822003042.
[25] X. Wang, B. Yang, J. You, Z. Gao, Coarse-fine adaptive tuned vibration absorber with high frequency resolution, J. Sound Vib. 383 (2016) 46–63, https://doi.org/10.1016/j.jsv.2016.07.030, https://www.sciencedirect.com/science/article/pii/S0022460X16303601.
[26] H. xia Deng, X. long Gong, Application of magnetorheological elastomer to vibration absorber, Commun. Nonlinear Sci. Numer. Simul. 13 (9) (2008) 1938–1947, https://doi.org/10.1016/j.cnsns.2007.03.024, https://www.sciencedirect.com/science/article/pii/S1007570407000524.
[27] H. Frahm, Device for damping vibrations of bodies, 1911.
[28] Y. Shen, Z. Xing, S. Yang, J. Sun, Parameters optimization for a novel dynamic vibration absorber, Mech. Syst. Signal Process. 133 (2019) 106282, https://

doi.org/10.1016/j.ymssp.2019.106282, https://www.sciencedirect.com/science/article/pii/S0888327019304972.
[29] K. Xu, T. Igusa, Dynamic characteristics of multiple substructures with closely spaced frequencies, Earthq. Eng. Struct. Dyn. 21 (12) (1992) 1059–1070, https://doi.org/10.1002/eqe.4290211203.
[30] T. Igusa, K. Xu, Vibration control using multiple tuned mass dampers, J. Sound Vib. 175 (4) (1994) 491–503, https://doi.org/10.1006/jsvi.1994.1341.
[31] H. Rice, Design of multiple vibration absorber systems using modal data, J. Sound Vib. 160 (2) (1993) 378–385, https://doi.org/10.1006/jsvi.1993.1033.
[32] J.M. Verdirame, S.A. Nayfeh, L. Zuo, Design of multi-degree-of-freedom tuned-mass dampers, in: G.S. Agnes (Ed.), Smart Structures and Materials 2002: Damping and Isolation, in: International Society for Optics and Photonics, vol. 4697, SPIE, 2002, pp. 98–108.
[33] L. Zuo, S. Nayfeh, Minimax optimization of multi-degree-of-freedom tuned-mass dampers, J. Sound Vib. 272 (3) (2004) 893–908, https://doi.org/10.1016/S0022-460X(03)00500-5.
[34] L. Zuo, S. Nayfeh, The two-degree-of-freedom tuned-mass damper for suppression of single-mode vibration under random and harmonic excitation, J. Vib. Acoust. 128 (2) (2006), https://doi.org/10.1115/1.2128639.
[35] F. Arnold, Steady-state behaviour of systems provided with nonlinear dynamic vibration, J. Appl. Mech. 22 (12) (1955), https://doi.org/10.1115/1.4011141.
[36] R.E. Roberson, Synthesis of a nonlinear dynamic vibration absorber, J. Franklin Inst. 254 (3) (1952) 205–220, https://doi.org/10.1016/0016-0032(52)90457-2.
[37] H. Ding, L.-Q. Chen, Designs, analysis, and applications of nonlinear energy sinks, Nonlinear Dyn. 100 (6) (2020), https://doi.org/10.1007/s11071-020-05724-1.
[38] S. Lin, Y. Zhang, Y. Liang, Y. Liu, C. Liu, Z. Yang, Bandgap characteristics and wave attenuation of metamaterials based on negative-stiffness dynamic vibration absorbers, J. Sound Vib. 502 (2021) 116088, https://doi.org/10.1016/j.jsv.2021.116088.
[39] N. Zhou, K. Liu, A tunable high-static–low-dynamic stiffness vibration isolator, J. Sound Vib. 329 (9) (2010) 1254–1273, https://doi.org/10.1016/j.jsv.2009.11.001, https://www.sciencedirect.com/science/article/pii/S0022460X09008918.
[40] C. Cai, J. Zhou, L. Wu, K. Wang, D. Xu, H. Ouyang, Design and numerical validation of quasi-zero-stiffness metamaterials for very low-frequency band gaps, Compos. Struct. 236 (2020) 111862, https://doi.org/10.1016/j.compstruct.2020.111862.
[41] H. Yao, Z. Chen, B. Wen, Dynamic vibration absorber with negative stiffness for rotor system, Shock Vib. 2016 (2016), https://doi.org/10.1155/2016/5231704.
[42] X. Sun, X. Jing, J. Xu, L. Cheng, Vibration isolation via a scissor-like structured platform, J. Sound Vib. 333 (9) (2014) 2404–2420, https://doi.org/10.1016/j.jsv.2013.12.025, https://www.sciencedirect.com/science/article/pii/S0022460X13010687.
[43] R. Ibrahim, Recent advances in nonlinear passive vibration isolators, J. Sound Vib. 314 (3) (2008) 371–452, https://doi.org/10.1016/j.jsv.2008.01.014.
[44] Q. Zhang, D. Guo, G. Hu, Tailored mechanical metamaterials with programmable quasi-zero-stiffness features for full-band vibration isolation, Adv. Funct. Mater. 31 (33) (2021) 2101428, https://doi.org/10.1002/adfm.202101428.
[45] S. Shan, S.H. Kang, J.R. Raney, P. Wang, L. Fang, F. Candido, J.A. Lewis, K. Bertoldi, Multistable architected materials for trapping elastic strain energy, Adv. Mater. 27 (29) (2015) 4296–4301, https://doi.org/10.1002/adma.201501708.
[46] O. Gendelman, Transition of energy to a nonlinear localized mode in a highly asymmetric system of two oscillators, Nonlinear Dyn. 25 (2001) 237–253, https://doi.org/10.1023/A:1012967003477.
[47] O. Gendelman, L. Manevitch, A. Vakakis, R. M'Closkey, Energy pumping in nonlinear mechanical oscillators: part I—dynamics of the underlying Hamiltonian systems, J. Appl. Mech. 68 (1) (2001), https://doi.org/10.1115/1.1345524.
[48] A. Vakakis, O. Gendelman, Energy pumping in nonlinear mechanical oscillators: part II—resonance capture, J. Appl. Mech. 68 (1) (2001), https://doi.org/10.1115/1.1345525.
[49] H. Li, Y. Li, J. Li, Negative stiffness devices for vibration isolation applications: a review, Adv. Struct. Eng. 23 (8) (2020) 1739–1755, https://doi.org/10.1177/1369433219900311.